

# Fault Tolerant Control for a Cluster of Rocket Engines – Methods and outcomes for guidance and control recovery strategies in launchers

**Nuno Paulino<sup>(1)</sup>, Cristina Roche Arroyos<sup>(1)</sup>, Luís Ferreira<sup>(1)</sup>, Matteo Pascucci<sup>(1)</sup>, Pedro Cachim<sup>(1)</sup>, Pedro Lourenço<sup>(1)</sup>, Jorge Arnedo García<sup>(2)</sup>, Diego Navarro-Tapia<sup>(3)</sup>, Andrés Marcos<sup>(3)</sup>, Mohamed Lalami<sup>(4)</sup>, Paul Alexandre<sup>(4)</sup>, Pedro Simplicio<sup>(5)</sup>, Samir Bennani<sup>(5)</sup>, Massimo Casasco<sup>(5)</sup>**

<sup>(1)</sup> GMV, Alameda dos Oceanos 115 1990-392, Lisboa, Portugal, +351 213829366, {nuno.paulino, cristina.roche, luis.ferreira, matteo.pascucci, pedro.cachim, palourenco}@gmv.com

<sup>(2)</sup> GMV, Isaac Newton 11, P.T.M. Tres Cantos, E-28760 Madrid, Spain, +34 918072100, jarnedo@gmv.com

<sup>(3)</sup> Technology for Aerospace Control (TASC) Ltd, 16 Stembridge, Martock, TA12 6BN, United Kingdom, diego.navarro-tapia@tasc-group.com, andres.marcos@tasc-group.com

<sup>(4)</sup> Société Anonyme Belge de Constructions Aéronautiques, Bruxelles, Belgium, +32 7295616, Mohamed.Lalami@sabca.be, Paul.alexandre@sabca.be

<sup>(5)</sup> ESA/ESTEC, Keplerlaan 1, 2201 AZ Noordwijk, Netherlands, +31 681094434, Pedro.Simplicio@ext.esa.int, samir.bennani@esa.int, Massimo.Casasco@esa.int

## ABSTRACT

Fault tolerant control for clusters of engines in launchers has re-gained attention due to recent capabilities of new reusable launchers. The redundancy in clusters of engines can be exploited to be robust against potential propulsion or thrust vector control failures that jeopardize mission success. The project “Fault-Tolerant Control of Clusters of Rocket Engines (FTC-CRE)” is an activity supported by the European Space Agency to demonstrate reconfiguration capabilities in case of propulsion and TVC failures for launch vehicles with cluster of engines. The outcomes of the activity are suitable requirements and methodologies for guidance and control architectures with embedded fault tolerant capabilities, and the increase of the readiness level for recovery strategies of stability and performance in the presence of failures. We provide an overview of the activity, aims and objectives, followed by the description of a test case of a launcher with a cluster of 5 thrusters during ascent, subjected to engine and TVC failures. We provide an analysis of how recovery strategies can mitigate for jamming and loss of power in the TVC and loss of thrust in the engines, and the applicability of successive convexification for trajectory reconfiguration and the optimal guidance problem with cluster of engines.

## 1 INTRODUCTION

Fault tolerant control for a cluster of engines in launchers has re-gained attention in recent times thanks to the development of capabilities of new reusable launchers such as SpaceX Falcon 9 and Starship. Most mission failures in the last quarter of the century were caused by loss of propulsion or failures in Thrust Vector Control (TVC). The former involves an off-nominal thrust delivery by the propulsion system that causes insufficient launch delta-V, leading to a failure to reach orbit or an off-nominal orbital injection performance. Moreover, in the case of TVC, a reduction in thrust also leads

to a reduction in control authority. The use of fault tolerant control (FTC) functions for launch vehicles is nowadays mostly passive, based on hardware redundancy (e.g. Ariane 5 launcher [1]), with the adoption of active FTC schemes very limited and mainly based on ad-hoc solutions (e.g. VEGA launcher [2]), and advanced control techniques such as the adaptive augmentation control scheme used by the SLS [3], which is shown to augment the envelope of the mission and avoid potential loss of vehicles. However, the redundancy provided by the cluster of engines can be intelligently exploited to mitigate failures that affect propulsion or thrust vectoring.

The project entitled “Fault-Tolerant Control of Clusters of Rocket Engines (FTC-CRE)” is an activity supported by the European Space Agency aimed at the demonstration of guidance and control (G&C) laws for launch vehicles with cluster of engines, with focus on reconfiguration capabilities in case of propulsion and TVC failures. The main outcome of the activity is the definition of the most suitable set of requirements and methodologies for a G&C architecture with embedded fault tolerant capabilities, and the increase of the readiness level for recovery strategies which ensure stability and performance in the presence of failures in the engines and actuators.

This work considers realistic, total and partial, failures in one of the cluster’s engines as well as thrust vectoring failures. Since the goal of the present activity is to develop fault-tolerant G&C algorithms, the considered failures are those that decrease the performance of the launcher but that are not considered catastrophic. The modelled failures simulated and analyzed are: **a)** partial and total loss of thrust in one engine; **b)** thrust vector actuator fixed at non-zero deflection in an outer engine (loss of communication, avionic failure or any jamming-like behavior); **c)** loss of power of the thrust vector actuator in an outer engine. The loss of thrust is modelled by introducing failures in oxidizer and fuel injection valves, whereas the actuator failures are simulated in a detailed multi-physics Simscape-based model of the TVC actuators.

The investigated recovery strategies rely on control reconfiguration and trajectory re-planning based on the detected failure. At the control level, the considered reconfiguration actions are: **a)** use an allocation algorithm to optimize thrust levels and deflections within the cluster to compensate for the loss of thrust, TVC failures and any induced parasitic torque; **b)** switch to a controller designed to be robust to the failure up to a certain tolerance level; **c)** explore the use of a more aggressive TVC inner-loop controller.

Reconfiguration of the control might not suffice to recover the requirements and it might be necessary to mitigate the failure at guidance level by performing a trajectory re-planning accounting for the available capability of the vehicle. The guidance trajectory generation problem encompasses nonlinear dynamics and several nonconvex state and control constraints. One approach that has been explored in recent literature for handling both nominal and reconfiguration launcher guidance is Successive Convexification (SCvx) [4]. This approach can address the nonconvex and nonlinear nature of the problem while making it amenable for closed-loop online implementation. However, the challenge of finding an optimal solution under the assumption of clustered actuation with throttleable and gimbaled thrusters and with adaptability in response to actuation faults is yet to be tackled in the literature. In this work, the SCvx scheme is employed to find a solution to the launcher trajectory generation problem. The guidance considers a 6-degrees-of-freedom model, incorporating unstable aerodynamics and a complex actuation model for the cluster of rocket engines with TVC actuators. Additionally, the guidance problem formulation includes a novel approach for robustness against the considered engine fault scenarios and for reconfiguration of the nominal trajectory.

This article provides an overview of the FTC-CRE activity and its main results, and the used simulation environment based on a test case of a launcher with a cluster of 5 engines during ascent, subjected to propulsion and TVC failures. The simulator includes the nonlinear dynamics, environment, and a developed detailed model of the TVC electro-mechanical actuator model TVC

failures. On this basis, a recovery decision logic is proposed relying on fault tolerant control and trajectory reconfiguration, and the recovery actions are tested and analyzed with the simulator.

The article is organized as follows: Section 2 provides a summary of the launching system, mission and the models to simulate the first stage test case in the presence of failures; Section 3 briefly describes the approach for the baseline nominal G&C, followed by the proposed recovery logic and a description of the recovery actions; Section 4 provides a summary of the test campaigns carried in the project and provides some of the results, followed by a discussion of the analysis carried during the activity; Section 5 summarizes the main points of the activity and conclusions.

## 2 MODELLING the SYSTEM and FAILURES

### 2.1 Application, system and mission

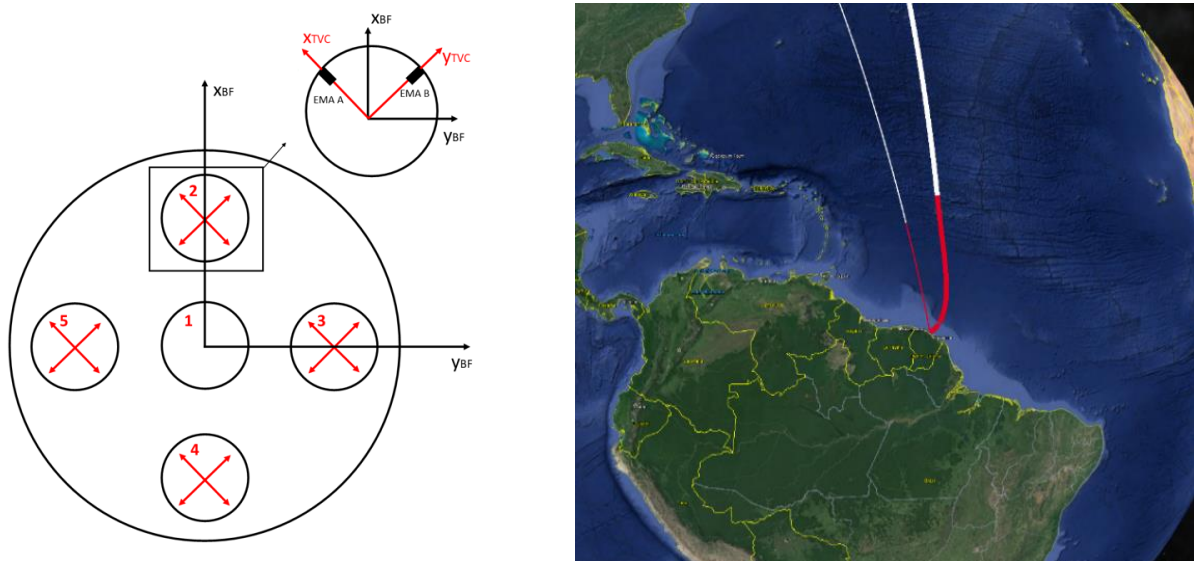


Figure 1. Configuration of the TVC actuators for the cluster of engines of the 1st stage with respect to the Body Frame (left) and flight trajectory (right)

The case study for the activity is the first stage of a small hybrid propellant rocket. The considered launcher is a two-stage-to-orbit kind of launch vehicle, where the first stage is propelled by a 5-engines cluster with cross-shaped arrangement and each of the engines is actuated by 2 TVC actuators, see left plot in Figure 1. The complete launcher has a length of 25 m and a diameter of 1.8 m and its gross lift-off mass is close to 33000 kg.

The reference trajectory has been generated with an internal trajectory optimization tool developed by GMV, using a nominal mission with the following characteristics. The objective orbit is a Sun Synchronous Orbit of 400 km of altitude with a 250 kg of payload. The optimization tool generates an optimal trajectory from Kourou Launch Base to reach the objective orbit minimizing the consumed fuel, see right plot in Figure 1. This reference trajectory is key for the nominal guidance of the 6DOF simulations carried out with the Simulator, as it is employed to generate the reference Look-Up Tables. The main requirements for the ascent mission are that the  $Q_{alpha}$  must be lower than 80 kPa°, to avoid severe aerodynamic forces affecting the launcher, and that the roll rate shall be lower than 5°/s, to approximate that the pitch and yaw attitude control channels are decoupled from the roll.

## 2.2 Functional Engineering Simulator

This chapter addresses the structure of the Functional Engineering Simulator (FES), where the G&C methods are implemented and tested for analysis.

The **Space Segment** in the FES contains the elements of the launcher and external elements that impact the launcher trajectory. It includes gravity gradient torque, the gravitational acceleration with J2 perturbation, the wind and atmospheric models, and the aerodynamic loads. The resultant forces and torques from the environment and actuation modules that impact the launcher attitude and translational dynamics and kinematics are used to integrate the state of the launcher, and also to compute the evolution of the MCI (Mass, Centre of mass and Inertia matrix). The navigation in FTC-CRE considers only behavioural navigation models to mimic the performance of a representative navigation filter and no sensor equipment is modelled.

Finally, we have models for the **Actuators**: the propulsion system, responsible for computing the thrust force and mass consumption; the thrust vector control actuator; and eight cold gas thrusters to control the roll rate. In particular, the TVC simulator consists of a Multiphysics Simscape model of an actuation system composed of two electromechanical actuators (EMAs), its control and power electronics and the power supply (battery). The model includes among others the permanent magnet synchronous motor, the gearbox and the ball screw, the power switches, sensors and the software controller and the nozzle dynamics. The healthy TVC behaviour has been validated against real test data of SABCA's EMAs. The failures considered in the test scenarios of this project are also implemented in the actuator's module. The TVC model can trigger and simulate faults of electrical or mechanical components in the system which lead to the loss of power or the stuck of an actuator.

The **On-board Software** (OBSW) receives information from the launcher state and is responsible to trigger the Guidance Navigation and Control (GNC) modes, computing of control commands for the actuators, and activating recovery actions in a faulty scenario. A **Launch Vehicle Manager** (LVM) function detects the mission events and decides on the GNC modes or functions. Additionally, it identifies and notifies the OBSW for specific events such as the second stage separation. The **Failure Detection Isolation and Recovery** (FDIR) function receives the telemetry from the TVC and the engines and triggers the recovery actions of the Guidance, TVC Control and TVC Dynamic Allocation. The detailed design of the **Navigation** function is not the focus of this activity, and the detailed definition of the sensors model and the navigation function is substituted by behavioural models which supply the non-gravitational velocity, attitude, attitude rates, position and velocity for use in control. The **Guidance** function is responsible for providing the launcher reference attitude (pitch and yaw angles) and reference velocity to the flight control, depending on the phase of the flight, as decided by the LVM. The **Control** function computes the TVC deflections and thrust levels necessary for attitude and trajectory tracking. It contains the sub-systems for control:

1. **TVC Control** – responsible for determining the torque that the TVC must apply to follow the reference guidance profile. It is responsible for rejecting disturbance as wind and sloshing effects that might destabilize the system, and contains the nominal and reconfiguration functions.
2. **TVC Allocation** – responsible for translating the torque input provided by the TVC control to the movements of the different actuators present in the TVC system. It also includes a nominal and a reconfiguration function triggered by the FDIR.
3. **Reaction Control System (RCS)** – This module is responsible for commanding the RCS cold gas thrusters, to limit the attitude rate. It provides on-off commands to the different thrusters based on their configuration.

## 2.3 Failure Scenarios

Table 1: Failure cases considered in the activity

| Description   | Failure type identifier |
|---|-------------------------|
| Loss of thrust in central engine below 40%            | F1                      |
| Loss of thrust in central engine above 40%            | F2                      |
| Loss of thrust in outer engine below 40%              | F3                      |
| Loss of thrust in outer engine between 40% and 70%    | F4a                     |
| Loss of thrust in outer engine above 70%              | F4b                     |
| Jamming of TVC at non-zero deflection in outer engine | F5                      |
| Loss of power of TVC in outer engine                  | F6                      |

The majority of mission failures in the last quarter of a century were caused by propulsion failures (50%), followed by GNC issues (15%, which includes actuator failures), and separation issues (5%). Based on the above trend, this activity considers the failure cases listed in Table 1.

In general terms and ignoring catastrophic failures (e.g. an engine chamber breach), propulsion failures involve an off-nominal thrust delivery by the propulsion system (*F1-F4*). In order to obtain a representative and quantifiable loss of thrust, the thrust reduction is modelled as a reduction in the mass flows of both oxidizer and fuel injectors, in the same amount, to reduce the total mass flow by a multiplicative factor.

In addition, two severe failures have been considered for the TVC actuator failures:

1. TVC jamming-like behavior (*F5*), modelled as one EMA stuck at a fixed non-zero position, leading to a non-zero deflection of one degree of freedom of one engine (one direction of its thrust).
2. The loss of power behavior (*F6*) is modelled as having one EMA free to move, leading to one degree of freedom of one engine uncontrolled. Misalignments result in force eccentricity and quasi-static acceleration, Figure 2, pushing the engine to one of its ends of stroke.

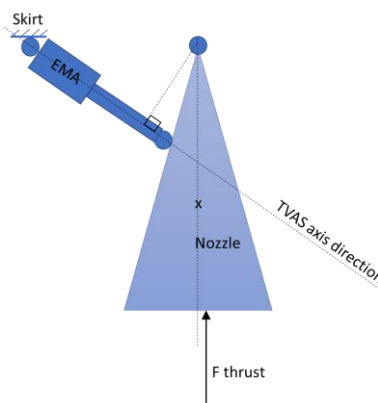


Figure 2. One axis TVC scheme, depicting the misalignment of the thrust direction which results in eccentric force.

## 3 FAULT-TOLERANT GUIDANCE and CONTROL DESIGN

### 3.1 Nominal guidance and control synthesis

Algorithms for guidance and control under *nominal* conditions (without failures) is designed and validated to provide a baseline to which we can compare the impact of the modelled failures, and the recovery strategies in terms of control authority, control performance, and dispersions at the end of the first stage flight. The nominal guidance uses an open-loop scheme scheduled with non-gravitational velocity, being the most used approach for endo-atmospheric on-board guidance consequence of its simplicity compared with closed-loop schemes. The guidance function is fed by the pitch and yaw profiles using look-up tables that were created using the reference generated with



the trajectory optimization tool. Regarding the control design, the synthesis uses specific operational points along the nominal trajectory, to obtain a linear structured  $\mathcal{H}_\infty$  controller with parameters which can be scheduled throughout the flight. The Linear Time Invariant (LTI) and Linear Fractional Transformation (LFT) mathematical models for design and robust analysis are defined for the linearized dynamics of the rocket launcher along points of the trajectory, under the usual assumptions of small angles and a gravity turn trajectory [5]. This control design approach has been widely used throughout the years for the purpose of rocket launchers robust control [6] due to the advantages offered by the  $\mathcal{H}_\infty$  framework, in terms of capabilities for robust control design and analysis for linear systems.

The LTIs and augmented plants are defined for each lateral channel to address attitude and drift control. The synthesis of the controller is performed by fine tuning the weighting functions of the augmented plant for a suitable tradeoff between control of attitude, drift and aerodynamic loads (weight on  $Q$  for the load relief of the vehicle [7]), while ensuring stability. After the synthesis, the LFTs are used with  $\mu$  analysis to check robust stability and performance against requirements under uncertainty. Finally, the nominal G&C is validated in the time domain with a Monte Carlo campaign and parametric dispersions with the FES.

The roll control is not a focus of the study, and a logic-based RCS is put in place to limit the roll rate using 8 cold gas thrusters placed symmetrically around the cross section. A bang-bang algorithm activates a pair or 4 of the thrusters when the roll rate exceeds its threshold.

Due to the cluster configuration of the engines, the application of the control torque is over-defined with redundant configurations of the deflections of the 4 outer nozzles. A nominal engine allocation unit decides the contribution of each of the engines to the total moment torque required for attitude and drift control. The allocation algorithm uses a high-efficiency quasi-linear algorithm based on a weighted Least Squares generalized inverse and augmented with a null-space method [8].

### 3.2 Recovery logic

Figure 3 illustrates the recovery logic scheme that combines the four recovery actions considered in the FTC-CRE activity (see Table 2) with the failures presented in Table 1. The *R1* recovery consists in a dynamic allocation function. This recovery approach will be complemented by an FTC  $\mathcal{H}_\infty$ -based approach to perform control reconfiguration under failure scenarios (*R2*). Another recovery action that will be explored in this activity is the change of TVC inner-loop control gains (*R3*) to reflect a temporary-stressed, but higher-performance TVC. Finally, guidance re-computation (*R4*) is meant to be the recovery action for those faults that cannot be handled by any of the above cases.

Table 2: Recovery actions considered in the activity

| Action identifier | Recovery action                                     |
|-------------------|---|
| R1                | Engine/TVC dynamic re-allocation                    |
| R2                | FTC controller with baseline TVC inner loop control |
| R3                | Aggressive TVC inner loop control                   |
| R4                | Guidance trajectory re-computation                  |

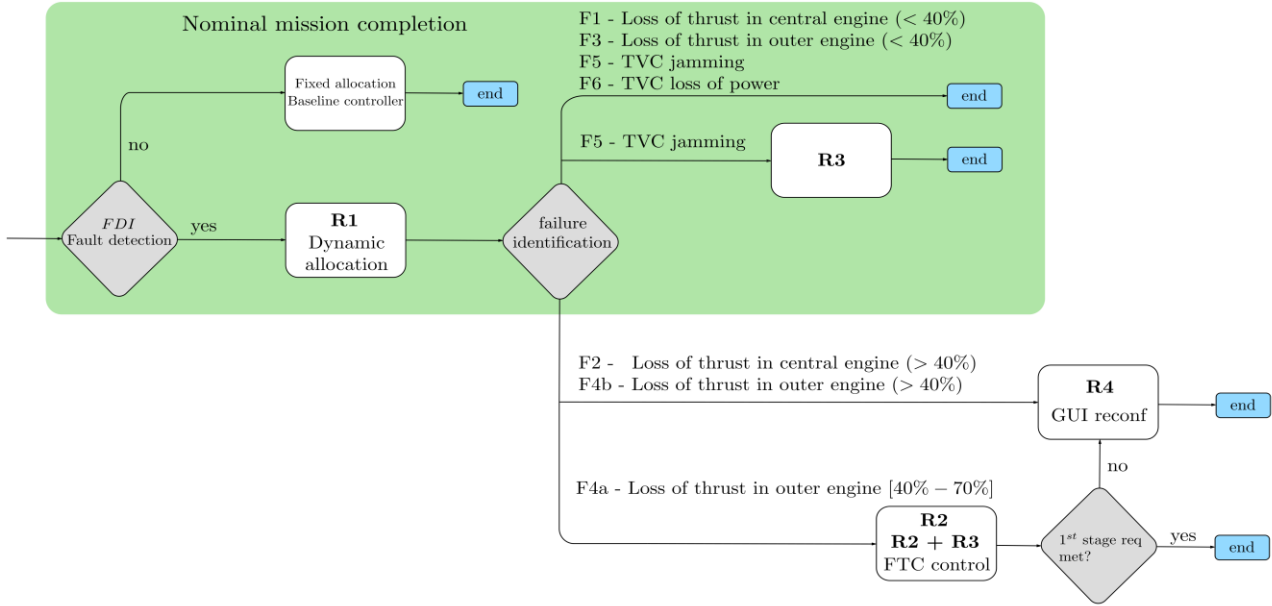


Figure 3. Recovery decision logic scheme

### 3.3 Dynamic allocation recovery (R1)

The use of dynamic TVC and engine thrust allocation is paramount in systems with multiple engines and TVC actuators. They can be used to obtain the necessary thrust levels and TVC deflections to follow the guidance trajectory, but also to perform reconfiguration under engine and/or TVC actuator failures.

Three different dynamic allocation functions have been explored in the framework of the *FTC-CRE* project. The first allocation function (*R1a*) solves the TVC and engine thrust allocation problems separately using failure information from the FDI function. The TVC allocation is solved using the pseudo-inverse solution, which was modified here for fault tolerant purposes. Also, in case of propulsion failures, *R1a* distributes the individual engine thrust levels based on the state of the healthy and faulty engines.

The other two dynamic allocation functions are based on optimization allocation algorithms that allow to jointly calculate the necessary thrust levels and TVC deflections to perform a recovery action while satisfying other constraints such as saturation or allowable thrust levels. In particular, *R1b* explores the use of convex-based optimization tools, whereas *R1c* uses non-linear optimization algorithms.

### 3.4 Fault Tolerant Control recovery (R2)

The recovery action *R2* aims to explore the advantages of replacing the nominal TVC controller by an FTC-based controller designed to be robust against propulsion failures. The FTC control design problem is formulated in the structured  $\mathcal{H}_\infty$  control framework using the closed-loop interconnection shown in Figure 4 that includes the key features for TVC launcher control design proposed in [9] and [10]. The design interconnection includes delay and TVC dynamics model ( $G_{TVC/delay}$ ), control allocation function (*CA*), wind disturbance inputs ( $v_{wu}$  and  $v_{wv}$ ), turbulence wind model that accounts for statistical severe wind levels ( $G_w$ ), rigid-body rotational and translational dynamics for both yaw and pitch dynamics ( $G_{LV}$ ) and tunable pitch and yaw controller blocks ( $K_\psi$  and  $K_\theta$ ).

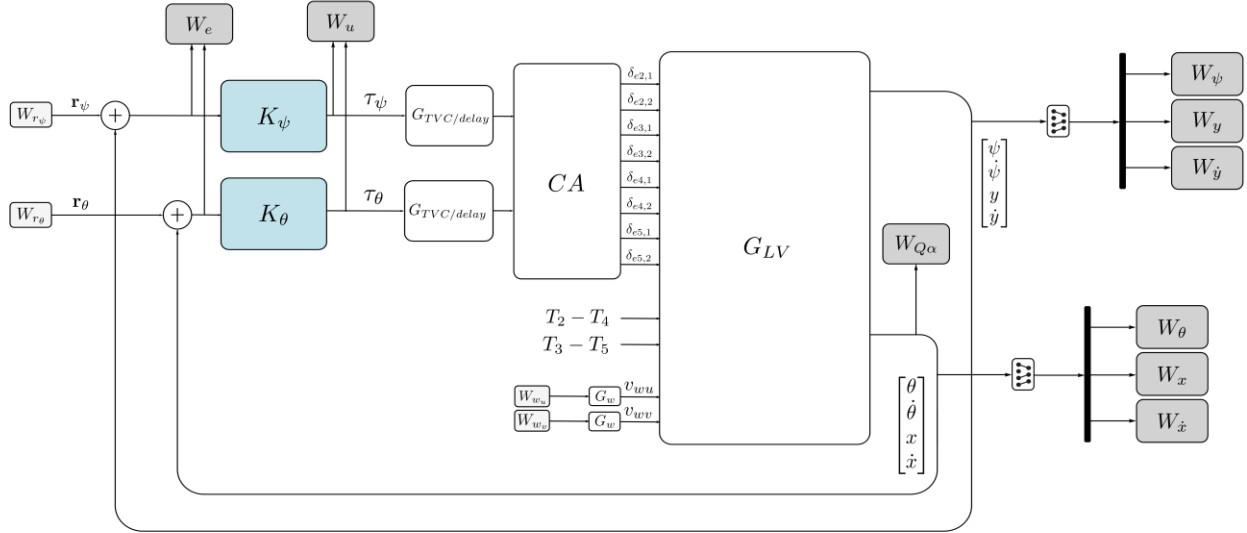


Figure 4. FTC closed-loop interconnection for design.

In addition, two important features have been considered for fault tolerant purposes. First, engine thrust failures can be explicitly considered in the synthesis process via modelling, and second, enforcing by design the minimization of the additional disturbance channel caused by the failure due to the mismatch between axis-symmetric engine thrust levels (e.g.  $T_2 - T_4, T_3 - T_5$ ).

The advantages of the above control formulation are exemplified via a design case considering a 60% loss of thrust failure in the outer engine 2 ( $F4a$ ). As presented in [11], the proposed robust control scheme can be effectively guided to favour specific trade-off performance objectives via proper choice of the design weighting functions. In this case, the main objective was selected to minimize the lateral deviation since this performance metric is significantly degraded by this specific failure.

### 3.5 Inner-loop TVC control recovery ( $R3$ )

The recovery action  $R3$  explores the use of TVC inner-loop control reconfiguration. For this purpose, a more aggressive TVC actuator model was tuned with a bandwidth increase of 70% (see Figure 5).

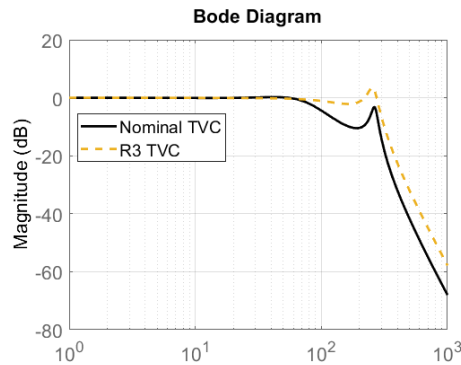


Figure 5. Nominal and R3 TVC models

### 3.6 Reconfiguration Guidance ( $R4$ )

Guidance reconfiguration ( $R4$ ) is triggered to compute a reconfigured trajectory by the LVM when the FDI informs of a thrust failure that lies into the  $R4$  recovery action paths, Figure 3. The FDI provides information on the loss of thrust that is used to configure the guidance model. Navigation state values are used as initial boundary conditions for the SCvx problem. The SCvx states are projected and adjusted to match the type of the nominal trajectory ones, so the obtained trajectory integration is the same as for the nominal trajectory. The reference trajectory is switched from the



nominal to the reconfigured one by the LVM. The reconfigured trajectory is scheduled in non-gravitational velocity to deal with model mismatching and environmental perturbations with a more robust approach.

The SCvx logic and problem formulation are based on [12] together with great contributions from [4] and [13]. The solution here presented is an efficient and tailored collection of different pieces of strategies selected in an optimal way for our problem plus self-developed contributions.

The reconfiguration guidance algorithm, also referred as to Recovery action 4 (*R4*), generates first stage flight trajectories using Successive Convexification (SCvx) and can model thrust module failures in the cluster of engines. Successive convexification for trajectory generation is often implemented by taking as an initial guess a trajectory defined interpolating the initial and final desired states. In contrast, this implementation leverages from having a preliminary trajectory, the nominal trajectory, that acts as an initial guess and thus providing a faster convergence rate. Unlike in the nominal trajectory, the flight phases are not imposed in the reconfiguration guidance and its triggering point is given by the LVM and FDI at the time occurrence of the failure. The guidance for reconfiguration provides a feasible and locally optimal trajectory around the nominal one and according to the new dynamics.

The flight trajectories exhibit maximum thrust continuously, not making use of the throttleable thrusters. Going at maximum thrust with a fixed available fuel determines the total flight time. Thus, SCvx problem can be defined in a fixed time formulation having a constant time step that does not dilate thus reducing both the optimization variables' space and the convergence time.

The kinematics and dynamics are defined in their non-convex, continuous-time formulation. The first stage is modelled as a rigid body subject to 6-DoF translational and rotational motion in Cartesian ECI, subject to a variable gravitational acceleration, aerodynamic normal and axial forces and torques. Mass changes as a function of the thrust, and thus forces and momentums change due to mass variability along the trajectory, making the thrust authority to change over time. Every iteration, the kinematics and dynamics are linearized around the previous iteration obtained trajectory and discretized, so the problem becomes a Linear Time-Varying (LTV) discrete system subject to state and control constraints and boundary conditions. The solution is found by minimizing the cost function at every iteration, transforming the original optimal non-linear control problem into a convex optimization problem with a solution that improves every iteration until a designed stop criterion. If the problem specifications are feasible, the states are well conditioned and the constraints are at maximum Second-Order Cone constraints, the solution is a feasible ascent trajectory locally optimal.

The linearization can result in constraints that admit an unbounded cost. To tackle this potential issue, the trust region and virtual control strategies are used. The trust region goal is to make the problem remain bounded in the process of the successive convexification, i.e., at each iteration ensure that each state value is chosen from a region where the linearization should be valid. Trust region requires the virtual control term in the problem definition to prevent artificial infeasibility. In the convergence process, there can happen that the linearization is not favourable for feasibility, i.e., satisfy states or control constraints, or that to satisfy them the solution needs to move further than the trust region constraint allows. In this case, the virtual control term absorbs the value of the states needed to satisfy the constraints.

The centre of pressure and mass are considered constant independent of the mass depletion. The centre of pressure of the launcher is closer to the nose than the centre of gravity, resulting in an unstable configuration. Therefore, the addition of the aerodynamic torque implies dealing with the unstable configuration of the launcher, i.e., aerodynamic torque increases in the same sense as the angle of attack does, therefore it is a torque which will increase any small deviation of the angle of attack around the 0 degrees.

The actuation is modelled to represent the geometry and power of a cluster of 5 engines, considering a central fixed engine and four perihelial gimbaled engines, see Figure 1 on the left. In case of a thrust failure, FDI information is provided, and guidance algorithm is reconfigured to model the loss of thrust in the faulty engine, and to increase the power of the other four to 110% capability, adapting the mass flow respectively. Exhaustion and atmospheric pressure contributions to the thrust are also modelled.

Each perihelial rocket engine is constrained by the maximum range of throwable thrust, the maximum gimbal angle and maximum gimbal angle rotational speed. Constraining the thrust to be constantly maximum is a non-convex constraint, and therefore needs to be relaxed as a maximum thrust constraint. This, together with the whole chosen definition of the problem transforms the thrust module constraint into a lossless constraint that can provide constant maximum thrust. Maximum allowed angular velocity is also imposed. As for boundary conditions, they are tailored for this problem in combination with the cost function, i.e., initial boundary conditions are imposed by the time occurrence of the failure and final boundary conditions are ensured by the cost function.

The goal of the reconfiguration guidance is to, disregarding the thrust failure conditions, reduce as much as possible the divergences at Main Engine Cut Off (MECO) to ensure that the second stage flight will be able to inject the payload into orbit, while respecting the system requirements on angle of attack and maximum dynamic pressure.

The chosen cost function includes penalization terms on the trust region for the states and control variables, and to minimize the virtual control. Besides, divergence from the final position is minimized and final velocity is maximized in a way that the angle of attack is minimized in the last timesteps. A proper tuning of the cost function allows for trajectory generation that fulfils the flight restrictions while converting the nominal original trajectory into a feasible one for the new faulty dynamics.

The problem at hand deals with optimization variables that cover very different orders of magnitude. In practice, numerical issues associated with sensitivity were observed. The scaling gains and offsets have been refined to uniform the problem. The obtained trajectories are tested end-to-end in the FES simulator to assess the validity of these assumptions. Open loop SCvx results replicate well the close loop results obtained with the FES, validating the representativity of the SCvx model and its tuning.

## **4 RESULTS and DISCUSSION**

### **4.1 Test Setup and Test Cases**

The verification and validation campaigns were carried out using the nonlinear functional engineering simulator described in Section 2.2, integrating the developed GNC and FTC functions. The simulations were performed considering: parametric dispersions on the properties of the launcher and environmental parameters; Earth gravity gradient torque; Earth higher order harmonics limited to J2; effect of the wind and turbulence; sloshing effect; navigation performance models; and the Multiphysics model of the TVC.

Table 3 provides the considered test cases, with identifiers given by MC-FX-N-RXXX where FX indicates the type of failure from Table 1, N defines the percentage of thrust loss, and XXX contain the digits of the combined recovery actions from Table 2. The campaign of baseline tests without failures or recovery actions is defined as MC-F0-0-R0. A single failure is triggered at the indicated time for the engine or the TVC, Table 3.

Test scenarios that include the guidance reconfiguration recovery action ( $R4$ ), consider a change of trajectory at the time occurrence of the failure, passing from the nominal to the reconfigured one that considers the fault dynamics. States values at the time of failure are the initial boundary conditions for the guidance model, and the reconfigured trajectory is provided by solving the optimization problem using successive convexification.

Table 3: Campaigns evaluated in the study

| Failure type | Modelling   | Actions triggered | Number of runs | Campaign identifier |
|--------------|---|-------------------|----------------|---------------------|
| -            | Nominal conditions and parameterisation   | -                 | 100            | MC-F0-0-R0          |
| F1           | Thrust reduction of 20%, in central engine, at time $t = 25$ s  | R1                | 100            | MC-F1-20-R1         |
| F3           | Thrust reduction of 20%, in outer engine number 2, at time $t = 25$ s   | R1                | 100            | MC-F3-20-R1         |
| F4a          | Thrust reduction of 60%, in outer engine number 2, at time $t = 25$ s of the simulation                                 | R1+R2             | 100            | MC-F4a-60-R12       |
|              |   | R1+R2+R3          | 100            | MC-F4a-60-R123      |
|              |   | R1+R2+R4          | 100            | MC-F4a-60-R124      |
| F5           | Jam in TVAS number 1 of outer engine number 2, at $t = 25.1$ s  | R1                | 100            | MC-F5-0-R1          |
|              |   | R1+R3             | 100            | MC-F5-0-R13         |
| F6           | Loss of power of TVAS number 1 of outer engine number 2, at $t = 25$ s, non-zero eccentricity, static disturbance force | R1                | 100            | MC-F6-0-R1          |
| F4b          | Thrust reduction of 100% , in outer engine number 2, at time $t = 25$ s of the simulation                               | R1+R4             | 100            | MC-F4b-100-R14      |
| F2           | Thrust reduction of 100% , in central engine , at time $t = 25$ s of the simulation                                     | R1+R4             | 100            | MC-F2-100-R14       |

## 4.2 Campaign Results

The different recovery actions are designed for different purposes: recover of control authority, control performance, or dispersions at MECO with respect to nominal. The purpose of these proposed metrics is to assess how each type of recovery action contributes in each of these purposes.

In this case, the control variables are used to assess control performance: drift, drift rate, pitch error and yaw error. The degradation of performance is checked in terms of system requirements by looking at the resulting limits in  $Q$ alpha and roll rate. First stage flight contribution to assist the second stage flight to achieve orbit injection is partially assessed by looking at the MECO divergences in position and velocity, described in RSW-like frame, which is centered at the nominal MECO, with the error in altitude (Radial) expressed in the x-axis, y-axis aligned with the cross-track (W-axis) and along-track direction using the z-axis (S-axis). It is important to remark, that the severity of a percentage of divergence in each component of position and velocity cannot be compared, since some combinations are more beneficial for the second stage flight.

*Note:* Due to restriction in length, the results included below concern only 4 of the campaigns with recovery strategies. However, in the discussion we include additional results obtained in the activity and the additional campaigns in Table 3.

### 4.2.1 MC-F6-0-R1 – Loss of power in TVC actuator of engine 2 using R1 recovery

The aim of the MC campaign MC-F6-0-R1 is to assess the effectiveness of the R1 recovery function to handle TVC loss of power failures. The results are shown in Figure 6, which shows the time-domain dispersion envelopes for the most relevant performance indicators of the launch vehicle during the ascent flight. Pitch and yaw errors, and corresponding drifts, are represented in the launcher body-frame, whereas each TVC deflection plot includes the two TVC deflections corresponding to that engine. Also note that the dispersion envelopes for the baseline non-faulty case (MC-F0-0-R0) are also displayed to serve as reference (see blue solid lines).

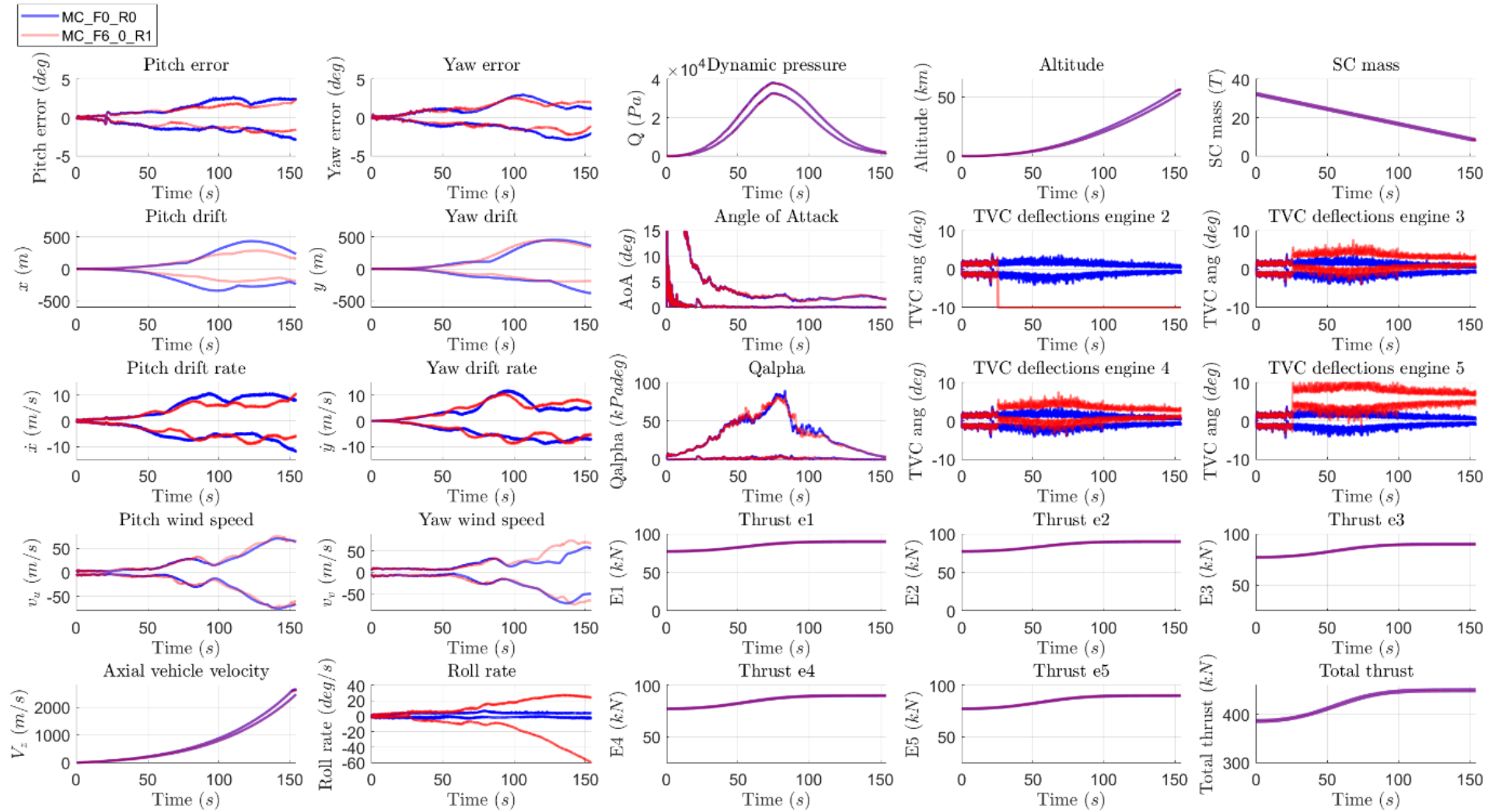


Figure 6. Envelopes of the time histories of the campaigns MC-F0-0-R0 and MC-F6-0-R1.

As shown in Figure 6, the TVC loss of power results in a large deviation of the faulty TVC actuator until reaching the TVC maximum deflection (i.e. 10 degrees), see red solid lines in TVC deflections engine 2 plot. The results show that *RI* provides recovery by performing dynamic TVC allocation (see different and higher TVC deflections for the faulty case). In addition, *RI* roughly presents the same range of dispersions for the main trajectory parameters (altitude, mass, thrust profile, axial vehicle velocity) as well as for the Qalpha profile. Also, *RI* further improves pitch attitude and drift responses with respect to the baseline non-faulty case. It is also observed that one of the TVC actuators of engine 5 reaches saturation in 13 cases. This aspect causes a significant degradation of the roll-rate responses for these cases.

Overall, the results show that the use of dynamic allocation approach are effective handling TVC actuator failures such as loss of power.

#### 4.2.2 MC-F4a-60-xx - Partial loss of thrust in outer engine 2 using different recovery actions

For some of the failure cases, different recovery strategies were tested. For instance, for propulsion failures above 40% (e.g. F4a in Table 1) three different combinations were explored: a) R1+R2; b) R1+R2+R3; c) R1+R2+R4. Figure 8 compares the time-domain dispersion envelopes for the most relevant performance indicators of the launch vehicle during the ascent flight for the aforementioned three recovery combinations. As before, the baseline non-faulty case (MC-F0-0-R0) is also displayed to serve as reference. Figure 8 illustrates that none of the recovery functions can reach the baseline non-faulty total thrust profile (see bottom-right plot), causing a reduction in the axial vehicle velocity. Also, the MECO dispersions obtained from the recovery functions are illustrated in Figure 7 and Figure 9.

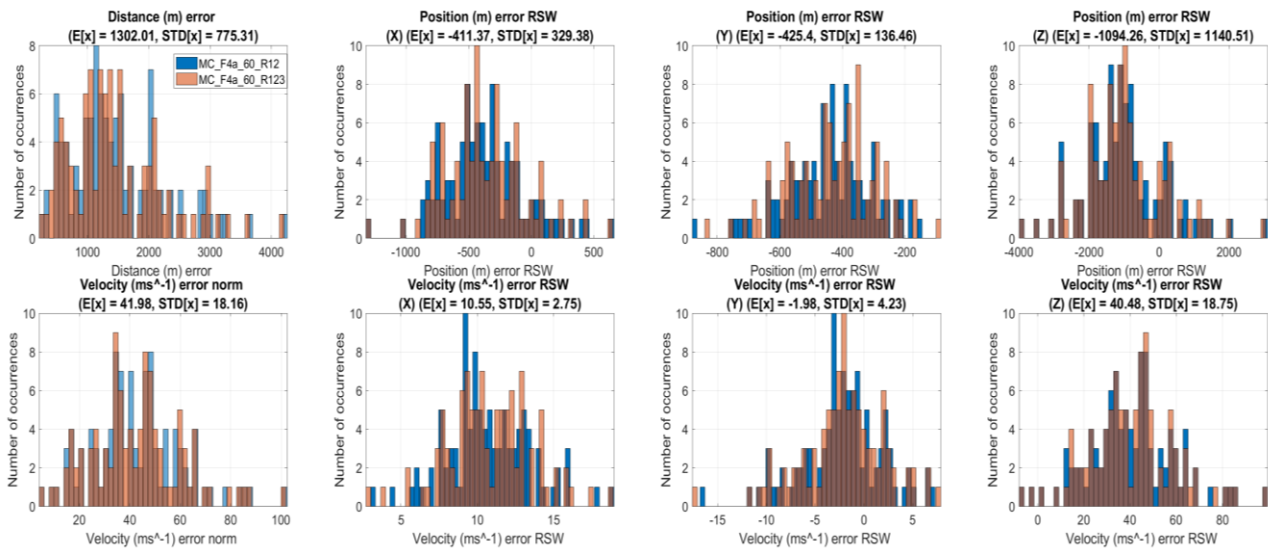


Figure 7. Comparison of the histograms of MECO dispersions the campaign MC-F4a-60-R123 and MC-F4a-60-R12. The values of  $E[x]$  and  $STD[x]$  are obtained for scenario MC-F4a-60-R123.



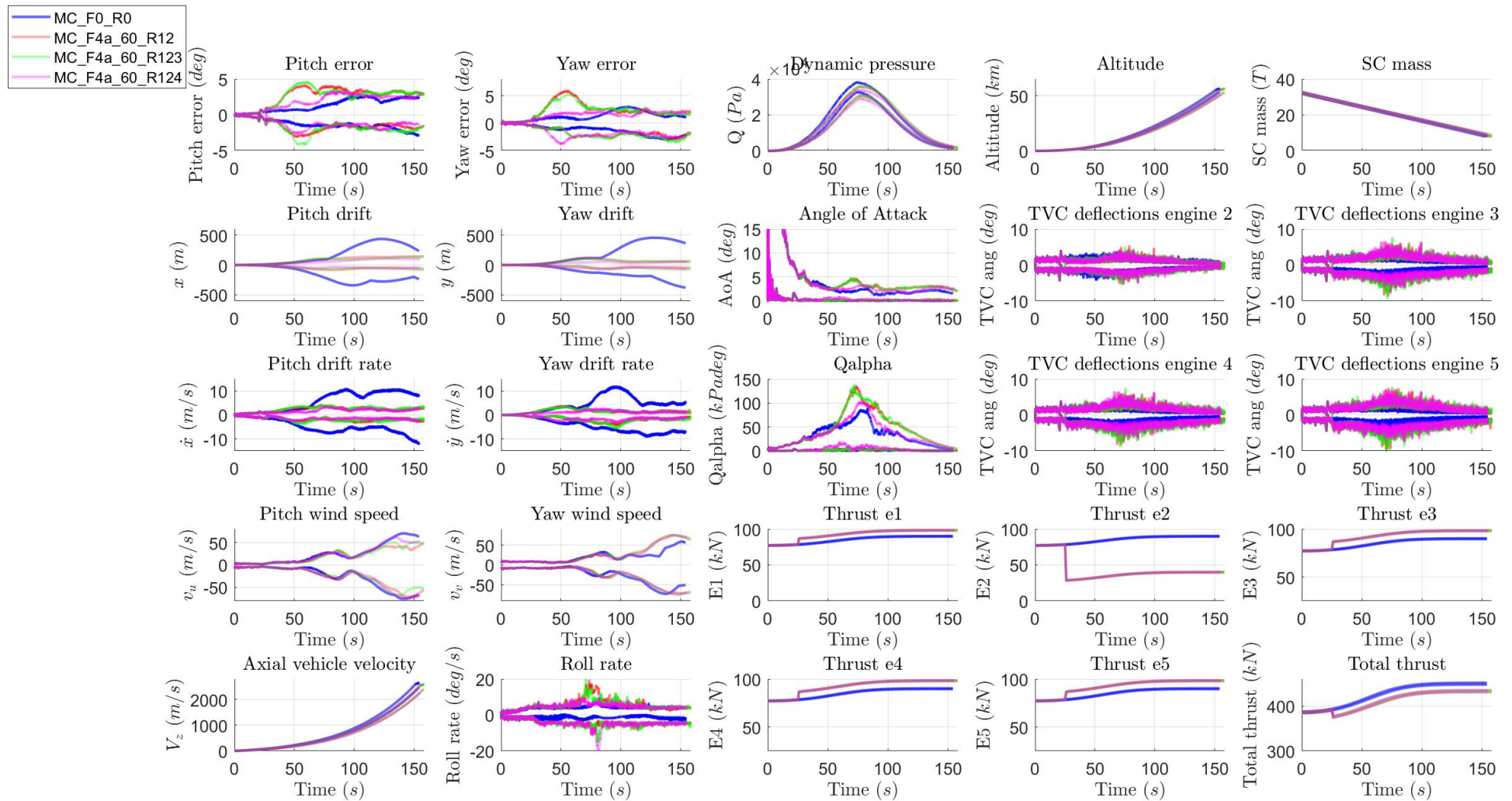


Figure 8. Comparison of the time history envelopes of the campaigns MC-F0-0-R0, MC-F4a-60-R12, MC-F4a-60-R123 and MC-F4a-60-R124.

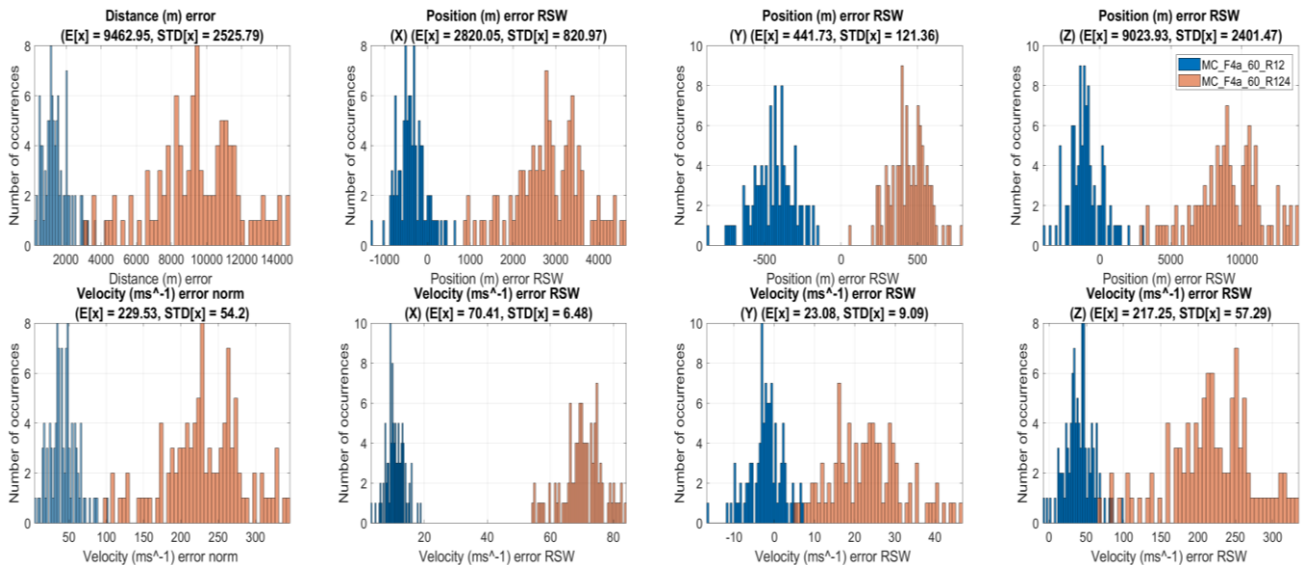


Figure 9. Comparison of the histograms of MECO dispersions the campaign MC-F4a-60-R124 and MC-F4a-60-R12. The values of  $E[x]$  and  $STD[x]$  are obtained for scenario MC-F4a-60-R124.

### 4.3 Discussion

The results from Section 4.2.1 show that dynamic TVC allocation approaches ( $R1$ ) can provide recovery from TVC actuator failures such as TVC loss power. Although not shown in this paper for compactness of presentation,  $R1$  can also provide recovery from propulsion failures up to 40% in a single engine (due to the 110% re-throttling constraint of the employed engines) as well as from other actuator failures such as TVC jamming.

Propulsion failures above 40% in a single engine cannot be compensated by  $R1$ , inevitably providing less thrust than the one commanded by the guidance profile. This in turn leads to a loss of velocity, which might hinder a successful orbital injection by the upper stages, but also leads to a significant performance degradation (e.g. attitude, lateral deviation, aerodynamic loads). While the former (i.e. loss of velocity) cannot be ameliorated unless increasing the throttling capabilities or redundancy of the engine cluster, the latter can be at least mitigated.

In this activity, three additional recovery functions have been explored to alleviate the performance degradation of the system under propulsion failures above 40%, see results from Section 4.2.2. The combination of  $R1$  and  $R2$  gathers the benefits of  $R1$  to alleviate the loss of thrust by increasing the throttling of the healthy engines at their maximum capacity and of  $R2$  that can provide robustness against the failure by design. In this activity,  $R2$  was designed to minimize the lateral deviations of the launch vehicle throughout the atmospheric ascent flight, but it is important to remark here that as shown in [11] the control design formulation proposed for  $R2$  can be tailored towards any of the other competing trade-off objectives during the ascent flight (e.g. attitude, drift, aerodynamic loads) or used to achieve a trade-off balance for the best global performance.

The introduction of  $R3$  (i.e.  $R123$ ) provides approximately the same responses as the  $R12$  recovery function, indicating that the increase of TVC inner-loop bandwidth does not have much impact on the system.

The use of a guidance reconfiguration ( $R4$ ) in combination with  $R1$  and  $R2$  (i.e.  $R124$ ) maintains the advantages of  $R12$ , that is, re-throttling of the healthy engines and significant lateral deviation reduction. The latter aspect is not trivial since changes in the guidance profile might conflict with the control function and alter the controller performance. In addition, it is also shown that  $R4$  provides a reconfigured trajectory that further improves key system requirements such as attitude and

aerodynamic loads presenting lower peaks at maximum  $Q_{\alpha}$  region. The obtained reconfigured trajectory considers the faulty dynamics and therefore seems to require lighter control action to follow the path. However,  $R4$  degrades the divergences achieved at MECO. With less thrust authority and no propellant mass margin,  $R4$  adapts the trajectory and makes it diverge from the nominal globally optimal one, at the price of worsening the final reached position and velocity that  $R1$  and  $R2$  were able to achieve.

The divergences observed at MECO in Figure 9 for 60% loss of thrust are worsened considerably in the case of a total loss of an engine (F4b and F2 in Table 3). In terms of system requirements, slightly worse results are obtained for the case of a lateral engine loss compared to a central engine loss. If this level of fault severity needs to be accounted for, the divergences at MECO need to be further assessed for mission feasibility with the compensation achieved by the flexibility of the second stage flight or by a readjustment of the propellant fuel margin for the first stage flight. Furthermore, a study on favorable combinations of states at MECO and its integration on the SCvx optimization would be able to favor a higher mission success rate at any level of divergences at MECO.

$R4$  was tuned for 70% loss of thrust in a lateral engine but could provide feasible trajectories for 100% loss of thrust, lateral engine scenarios, or scenarios with perturbations. It shows that  $R4$  tuning was not overfitted for a faulty case scenario and the optimization problem can be formulated in a flexible manner, that while obtaining local optimality is able to prioritize feasibility. For an improvement in the performance,  $R4$  can be tuned for each different regime and scenario.

Roll dynamics have been an important source of issues in the scenarios with perturbations since G&C algorithms model the roll as decoupled, and mismatching is generated.

## 5 CONCLUSION

This article presents the project “Fault-Tolerant Control of Clusters of Rocket Engines” which studied the reconfiguration capabilities during ascent of the first stage of a launcher test case, with a cluster of 5 thrusters. It describes a selection of failures in engine and TVC actuation, used to test recovery strategies which mitigate for jamming and loss of power in the TVC and loss of thrust in the engines. The failure scenarios are selected and modelled to evaluate the effectiveness of the different recovery fault-tolerant G&C strategies, in isolation or combined, with respect to the nominal operation.

This article explores the use of optimization of thrust levels and deflections within the cluster to compensate for the loss of thrust, TVC failures and any induced parasitic torques; the use of a controller designed to be robust to the failure up to a certain tolerance level; and the possibility of more aggressive TVC inner-loop controllers. It also demonstrates the use of closed-loop trajectory reconfiguration to exploit the redundancy in the cluster of engines, and the conditions where successive convexification for the optimal guidance problem is suitable. The analysis of the results provides the level of system degradation up to which control reconfiguration can be applied, and from which a trajectory re-planning/re-targeting needs to be performed. The SCvx guidance model under thrust failures has been proved to replicate the FES simulator close loop dynamics and have a sufficient representativity to make it suitable.

The different recovery strategies were compared with the nominal dispersions and performance, to understand the capacity to recover control authority, control performance and dispersions at main engine cut off. The outcomes of the activity provide insight on the capacity of clusters of engines for recovery, methodologies for guidance and control architectures with embedded fault tolerant capabilities, and their demonstration to increase of the readiness level for recovery strategies of stability and performance in the presence of failures.

## 6 ACKNOWLEDGEMENTS

This work is part of the project “Fault tolerant control of clustered rocket engines” (FTC-CRE) under a programme of, and funded by, the European Space Agency, Contract No. 4000136228/21/NL/CRS. The view expressed in this paper can in no way be taken to reflect the official opinion of the European Space Agency.

## 7 REFERENCES

- [1] Miramont P., “Ariane 5 on board software: redundancy management”, in *Proceedings of the 2nd Embedded Real Time Software Congress*, 2004.
- [2] Giannini M. and Cruciani I., “VEGA LV Qualification process: GNC aspects on HWIL testing and analysis”, in *Proceedings of the 5th European Conference for Aeronautics and Space Sciences*, 2013.
- [3] Orr J. S. and VanZwieten T. S., “Robust, practical adaptive control for launch vehicles”, in *Proceedings of the AIAA Guidance, Navigation, and Control Conference. American Institute of Aeronautics and Astronautics*, 2012.
- [4] Miao X., et al. "Successive Convexification for Ascent Trajectory Replanning of a Multistage Launch Vehicle Experiencing Nonfatal Dynamic Faults", *IEEE Transactions on Aerospace and Electronic Systems* 58.3, 2039-2052, 2021.
- [5] Barrows T., and Orr J.S., *Dynamics and Simulation of Flexible Rockets*, Academic Press, 2020.
- [6] Navarro-Tapia D., et al., “Structured H-infinity control design for the Vega launch vehicle: recovery of the legacy control behaviour”, in *Proceedings of the 10th International ESA Conference on Guidance, Navigation and Control Systems (ESA-GNC)*, 2017.
- [7] Simplicio P. et al., “New control functionalities for launcher load relief in ascent and descent flight”, in *Proceedings of the 8th European Conference for Aeronautics and Aerospace Sciences*, vol. 10, 2019.
- [8] Orr J. S. and Slegers N.J., “High-Efficiency Thrust Vector Control Allocation”, *Journal of Guidance, Control, and Dynamics*, Vol. 37, No. 2, 2014.
- [9] Navarro-Tapia D., et al, “Legacy Recovery and Robust Augmentation Structured Design for the VEGA Launcher”, *International Journal of Robust Nonlinear Control*; 29:3363-3388, 2019.
- [10] Navarro-Tapia D, “*Robust and Adaptive TVC Control Design Approaches for the VEGA Launcher*”, PhD thesis, University of Bristol, 2019.
- [11] Navarro-Tapia D., et al. “Performance and robustness trade-off capabilities for the VEGA Launcher TVC System”, in *Proceedings of the 8th European Conference for Aeronautics and Aerospace Sciences*, 2019.
- [12] Reynolds, T.P., et al. "Dual quaternion-based powered descent guidance with state-triggered constraints", *Journal of Guidance, Control, and Dynamics*, 2020.

[13] Szmuk M. and Acikmese B., "Successive convexification for 6-DOF Mars rocket powered landing with free-final-time", in *Proceedings of AIAA Guidance, Navigation, and Control Conference*, 2018.